Tellus (1988), *40A*, 407–418

A unified geostrophic equation with application to a cold core ring

By H. HUKUDA* and T. YAMAGATA, *Research Institute for Applied Mechanics, Kyushu University, Kasuga 816, Japan*

(Manuscript received 4 May 1987; in final form 29 February 1988)

ABSTRACT

The present paper considers a possible extension of previous work on intermediate geostrophic (IG) dynamics and an application to the Gulf Stream cyclonic ring. We generalize the IG equation to the degree at which either total energy or potential enstrophy of a reduced-gravity shallow water fluid system is conserved in time. Some progress is made in this respect and an evolution equation is derived via a perturbation approach using a high-order expansion in the Rossby number. The energy integral expression contains an ageostrophic term which is cubic in the geopotential function and suggests an asymmetric evolution of positive and negative IG vortices. We attempt to model the satellite-observed motions of a cyclonic Gulf Stream ring by using our approximate equation. The result for this example shows the present model to be superior to the quasi-geostrophic model.

1. Introduction

There are two ways by which one may eliminate the occurrence of undesirable inertial gravity waves in numerical predictions of large-scale atmospheric and oceanic phenomena. The use of the quasi-geostrophic equation (Charney, 1948), on the one hand, and that of the balance equation (Charney, 1955; Bolin, 1956), on the other hand, have been proposed to attain this purpose. In particular, the quasi-geostrophic equation has been extensively used in the literature. The equation represents an approximate equation, but exactly conserves both analogues of energy and enstrophy like the primitive equations. This characteristic seems to be one of the reasons for its successful application to atmospheres and oceans. The balanced model also has been extended to conserve total energy (Lorenz, 1960).

Current activities in this field may conveniently be divided into two categories. The first approach to study large-scale geophysical fluid motions is to find a slow manifold while solving the primitive equations (Leith, 1980; Lorenz, 1986). The second approach is to use the filtered models such as quasi-geostrophic equations (Pedlosky, 1979) or balance equations (Gent and McWilliams, 1983a, b). The present paper addresses the latter issue and proposes new geostrophic equations which conserve an analogue of either energy-like or enstrophy-like quantity.

In recent years, new dynamical regimes other than the quasi-geostrophic (QG) regime have been discovered [e.g., the intermediate geostrophic (IG) regime (Charney and Flierl, 1981; Yamagata, 1982); the planetary geostrophic (PG) regime (Williams and Yamagata, 1984); the frontal geostrophic (FG) regime (Cushman-Roisin, 1986)]. These findings naturally motivate a unification and generalization of previous studies (GG equation; see Cushman-Roisin, 1985; Williams, 1985). However, there is a possibility that these equa-

* Present affiliation: *Department of Physics and Newfoundland Institute for Cold Ocean Science, Memorial University of Newfoundland, St. John's, Newfoundland, Canada, A1B 3X7.*

tions, other than the quasi-geostrophic equation, may not correctly describe the conservation laws possessed by the original fluid systems. This mainly occurs in the process of making approximations to the primitive equation. Recently, Salmon (1985) derived a new geostrophic equation for large-scale flows (relative to Rossby deformation scale). Salmon's equation exactly conserves the total energy because his analysis is based on Hamilton's principle.

In the present paper, we attempt to generalize the IG dynamics to the degree at which either total energy or enstrophy of a shallow water fluid system is conserved in time. The parameter constraint we place on the dynamics is that Rossby, stratification and beta numbers are all small and of the same order. Progress is made in this respect and an evolution equation similar to Salmon's equation is derived via a systematic perturbation approach. It is also shown that the energy integral has an ageostrophic term (cubic in geopotential function) which suggests the asymmetric behavior of positive and negative IG vortices. The latter part of this paper is devoted to a study of modelling the satellite-observed motions of a cyclonic Gulf Stream ring by using our equations for nearly geostrophic motion. Advantages and limitations of the model are finally discussed.

2. A unified geostrophic equation

2.1. *An approximate equation*

We consider a two-layer model in which the upper layer lies on the deep motionless lower layer. The equations governing the upper layer motion are written as

$$u_t + uu_x + vu_y - fv = -g^* d_x, \tag{2.1}$$

$$v_t + uv_x + vv_y + fu = -g^* d_y, \tag{2.2}$$

$$d_t + ud_x + vd_y + d(u_x + v_y) = 0, \tag{2.3}$$

where u and v are the depth-averaged velocities, d the upper layer depth, f the local Coriolis parameter and g^* the reduced gravity. If the reference latitude is λ on a planet with the angular velocity Ω and the radius R, the beta-plane approximation yields

$$f = f_0 + \beta^* y, \tag{2.4}$$

where $f_0 = 2\Omega \sin\lambda$ and $\beta^* = 2\Omega \cos\lambda / R$. Furthermore, we consider an isolated perturbation of the fluid layer so that

$$d = d_0 + h(x, y, t), \tag{2.5}$$

where d_0 is a constant depth at infinity and h is the local perturbation height taken to be positive (negative) for a warm (cold) core eddy. We make a dimensionless set of basic equations by using the scalings $[U, L, L/U]$ for horizontal velocities, horizontal length and advection time scale. The scale for h is taken to be $f_0 UL/g^*$ from the geostrophic relation. Thus we introduce the nondimensional variables (shown with primes) as follows:

$$\left.\begin{aligned} (x, y, t, u, v) &= [Lx', Ly', (L/U)t', Uu', Uv'], \\ d &= d_0[1 + (\varepsilon/s)h'], \\ f &= f_0(1 + \beta y'). \end{aligned}\right\} \tag{2.6}$$

Here three dimensionless numbers are defined by

$$\beta = \beta^* L / f_0, \tag{2.7a}$$

$$\varepsilon = U/(f_0 L), \tag{2.7b}$$

$$s = g^* d_0 / (f_0 L)^2, \tag{2.7c}$$

which are called the beta, Rossby and stratification numbers, respectively. A dimensionless set corresponding to (2.1)–(2.3) is written, after dropping the prime,

$$\varepsilon(u_t + uu_x + vu_y) - (1 + \beta y)v = -h_x, \tag{2.8}$$

$$\varepsilon(v_t + uv_x + vv_y) + (1 + \beta y)u = -h_y, \tag{2.9}$$

$$\varepsilon(h_t + uh_x + vh_y) + (s + \varepsilon h)(u_x + v_y) = 0. \tag{2.10}$$

The purpose of the subsequent analysis is then to seek an evolution equation which governs geostrophic motions in a form as general as possible. For this purpose, we shall consider the following parameter range:

$$s, \beta = O(\varepsilon) \ll 1. \tag{2.11}$$

This parameter constraint may perhaps be relaxed to include the quasi-geostrophic range $s \leqslant 1$. However, we find that the asymptotic limit (2.11) is useful and greatly simplifies the subsequent analysis. If we choose the Rossby number as the appropriate ordering parameter, the dependent variables are then decomposed into a geostrophic part of O(1) and an ageostrophic part of O(ε). Thus, we write

$$u = -\phi_y + \varepsilon u_a, \tag{2.12}$$

$$v = \phi_x + \varepsilon v_a, \tag{2.13}$$

$$h = \phi + \varepsilon \phi_a. \tag{2.14}$$

From (2.8) and (2.9), keeping only dominant physical terms of order ε (linear with Rossby number), we obtain ageostrophic velocity components:

$$v_a = -\phi_{yt} - j(\phi, \phi_y) - By\phi_x + \phi_{ax}, \tag{2.15}$$

$$u_a = -\phi_{xt} - j(\phi, \phi_x) + By\phi_y - \phi_{ay}, \tag{2.16}$$

where $j(a,b) = \partial(a,b)/\partial(x,y)$ and $B = \beta/\varepsilon \sim O(1)$. Using (2.12)–(2.16), we obtain

$$u_x + v_y = -\varepsilon[\nabla^2\phi_t + j(\phi, \nabla^2\phi) + B\phi_x], \tag{2.17}$$

$$uh_x + vh_y = -(\varepsilon/2)[|\nabla\phi|_t^2 + j(\phi, |\nabla\phi|^2)], \tag{2.18}$$

where $\nabla = (\partial_x, \partial_y)$. On substituting (2.17) and (2.18) into (2.10), we find an evolution equation which predicts the time rate of change of the upper layer depth. This equation is written:

$$\begin{aligned}&\phi_t + \varepsilon\phi_{at} - (s + \varepsilon\phi)\nabla^2\phi_t - (\varepsilon/2)|\nabla\phi|_t^2 \\ &\quad - B(s+\varepsilon\phi)\phi_x - (s+\varepsilon\phi)j(\phi, \nabla^2\phi) \\ &\quad - (\varepsilon/2)j(\phi, |\nabla\phi|^2) = 0.\end{aligned} \tag{2.19}$$

Eq. (2.19) is a potential vorticity equation as a leading-order approximation in the Rossby number. Similar equations have been derived by Cushman-Roisin (1985) and Williams (1985), who, however, ignored the $O(\varepsilon)$ terms in time derivatives by assuming that the quasi-geostrophic components $(\phi - s\nabla^2\phi)_t$ dominate. The quasi-geostrophic system, as the asymptotic theory of (2.19) in the limit $\varepsilon \to 0$, exactly conserves both analogues of total energy and potential enstrophy (Pedlosky, 1979). In our opinion, one may seek, by another method, an evolution equation that has two global invariants for conservative flow, namely energy-like and enstrophy-like quantities, to higher order Rossby number. This attitude is basically the same as that taken by Salmon (1985) who derived a new geostrophic equation for large-scale flows on the basis of Hamilton's principle. Such a possibility will be next examined.

2.2. *A new equation*

The approach taken by Hoskins (1975) and Salmon (1985) proved to be a good one for reasons that will be shown shortly. We thus introduce the geostrophic coordinate transformation:

$$X = x + \varepsilon\phi_x, \tag{2.20a}$$

$$Y = y + \varepsilon\phi_y, \tag{2.20b}$$

$$T = t. \tag{2.20c}$$

From (2.20), it follows that

$$j(a,b) = (1 + \varepsilon\nabla^2\phi)J(a,b), \tag{2.21}$$

$$\phi_t = [\phi + (\varepsilon/2)|\nabla\phi|^2]_T, \tag{2.22}$$

to leading order in ε, where now $J(a,b) = \partial(a,b)/\partial(X,Y)$ and $\nabla = (\partial_X, \partial_Y)$. Applying (2.20), (2.21) and (2.22) to (2.19), we see that the equation in the transformed coordinates takes the asymptotic form (see Appendix A for more details).

$$\begin{aligned}&[\phi + \varepsilon\phi_a - (s+\varepsilon\phi)\nabla^2\phi]_T - B(s+\varepsilon\phi)\phi_X \\ &\quad - (s+\varepsilon\phi)J(\phi, \nabla^2\phi) - (\varepsilon/2)J(\phi, |\nabla\phi|^2) = 0.\end{aligned} \tag{2.23}$$

Eq. (2.23) is the desired one: the time derivative is now written as $\partial Q/\partial T$ where Q is some quantity, whereas eq. (2.19) does not have such a character, because there is a missing term, i.e., $-\varepsilon\phi_t\nabla^2\phi$. In fact, our motivation for obtaining a new equation was to recover the missing term and this is the main reason why we must perturb the coordinates. The approximated eq. (2.19) falls short of describing any conservative quantities other than the total volume.

There is an arbitrariness in eq. (2.23). The ageostrophic height ϕ_a must be determined. It is a reasonable idea that the requirement of energy conservation may determine it. Thus, we will consider the boundary conditions so that a perturbation field vanishes at infinity ($\phi \to 0$, at $X, Y \to \infty$), or that ϕ is periodic in both X and Y. Multiplying (2.23) by ϕ and integrating over the entire region yields:

$$\begin{aligned}&\iint \phi[\phi + \varepsilon\phi_a - (s+\varepsilon\phi)\nabla^2\phi]_T \,\mathrm{d}X\,\mathrm{d}Y \\ &\quad = \tfrac{1}{2}\iint (\phi^2 + s|\nabla\phi|^2 + 2\varepsilon\phi|\nabla\phi|^2)_T \,\mathrm{d}X\,\mathrm{d}Y \\ &\quad + \iint \varepsilon\phi[\phi_a + \tfrac{1}{2}|\nabla\phi|^2]_T \,\mathrm{d}X\,\mathrm{d}Y = 0.\end{aligned} \tag{2.24}$$

For a measure of total energy to be conserved, a constraint must be placed on the last integral in (2.24). There is still some arbitrariness and we will consider only one possibility.

The natural choice is to set

$$\phi_a = -\tfrac{1}{2}|\nabla\phi|^2. \tag{2.25}$$

Eq. (2.23) is then rewritten as

$$Q_T + J(\phi, \pi) = 0, \tag{2.26}$$

where

$$Q = \phi - (\varepsilon/2)|\nabla\phi|^2 - (s + \varepsilon\phi)\nabla^2\phi, \tag{2.27}$$

$$\pi = Q - (s + \varepsilon\phi)BY. \tag{2.28}$$

We may verify that eq. (2.26) with (2.27) and (2.28) is the same as eq. (4.15) in Salmon's paper (Salmon's notation differs somewhat from ours, but we can easily identify both equations if h_s and Φ_s^* in his paper are replaced by Q and ϕ, respectively and also f is expanded in powers of small beta number). However, this is not a satisfactory result since eq. (2.26) does not take a form to conserve π which we identify as the inverse potential vorticity. We are therefore forced to generalize eq. (2.26) to the form for which the potential vorticity may be materially or globally conserved. This amounts to taking the ageostrophic currents into consideration. First, one may define the modified geopotential ψ (which incorporates the beta term) as

$$(1 + \beta Y)\psi_X = \phi_X, \tag{2.29a}$$

$$(1 + \beta Y)\psi_Y = \phi_Y, \tag{2.29a}$$

Then, instead of (2.26), one obtains

$$\pi_T + J(\psi, \pi) = 0. \tag{2.30}$$

Eq. (2.30) states that the inverse potential vorticity π is materially conserved following geostrophic currents. Moreover, it generates an infinite number of conserved quantities (π^n, $n = 1, 2, \ldots$). It is like Salmon's potential vorticity equation [eq. (4.16) in his paper; note that h_s/f_s in his notation is equivalent to π here (see below)].

Let us now consider a physical meaning of π. If we expand the inverse potential vorticity function in power of the Rossby number, it may be shown that:

$$\frac{d}{f + \zeta} \simeq \frac{d_0}{f_0} + \frac{UL}{g^*}\{\phi + \varepsilon\phi_a - (s + \varepsilon\phi)(\nabla^2\phi + By)\}, \tag{2.31}$$

where ζ represents the relative vorticity, $v_x - u_y$. With the constant factors omitted, it is just π, provided the ageostrophic height is given by (2.25). The reason why we must consider the inverse potential vorticity is clear because we can not expand $1/d$ due to the constraint $s = O(\varepsilon)$. This is contrasted with the quasi-geostrophic approximation in which the depth is expanded around a mean state. Another difference is shown in the expression of the energy integral. From (2.24) and (2.25), it follows that eq. (2.26) conserves the total energy

$$E = \tfrac{1}{2}\iint (\phi^2 + s|\nabla\phi|^2 + 2\varepsilon\phi|\nabla\phi|^2)\,dX\,dY \tag{2.32}$$

in time. The first two terms and the third term in brackets represent the quasi-geostrophic and ageostrophic parts of the total energy, respectively. The last term is of cubic form and there is therefore asymmetry between cyclonic and anticyclonic eddies, a phenomenon which is absent in quasi-geostrophic dynamics. The sign of this extra term is definitely positive for anticyclones and negative for cyclones. This is suggestive of an asymmetric evolution of anticyclonic and cyclonic eddies found by Matsuura and Yamagata (1984).

It seems, at first, that the above remarks only apply to a transformed system. A remarkable coincidence exists, however, of both physical and geostrophic coordinates systems. By taking the inverse transformation and applying it to (2.26), one may show that the equation remains the same if ϕ in (2.26) is replaced by the total height h and the physical coordinates are referred to (see Appendix A). The asymmetric property mentioned above is therefore an inherent dynamics, not a spurious feature introduced by the transformation. The whole story is, of course, based on how we can cope with the errors in $O(\varepsilon^2)$.

Although Salmon's equation appears to be a unique one, its solution has not been found yet. Therefore we look for a modified equation which is easily solvable by standard numerical methods. For this purpose, we consider the following model equation:

$$Q_T^* + J(\phi, \pi^*) = 0, \tag{2.33}$$

where

$$Q^* = \phi - |\nabla\phi|^2 - (s + \varepsilon\phi)\nabla^2\phi, \tag{2.34}$$

$$\pi^* = Q^* - (s + \varepsilon\phi)BY. \tag{2.35}$$

Eq. (2.33) is equivalent to one which incorporates ageostrophic currents as well as geostrophic flows in advection terms. Namely, it can be derived from (2.26) by replacing ϕ with ϕ^* where ϕ^* is defined as

$$\phi_X^* = \phi_X - \varepsilon\{\phi_{YT} + J(\phi, \phi_Y)\}, \tag{2.36a}$$

$$\phi_Y^* = \phi_Y + \varepsilon\{\phi_{XT} + J(\phi, \phi_X)\}, \tag{2.36b}$$

A nice feature of eq. (2.33) is that it conserves an analogue of the enstrophy-like quantity

$$F = \iint Q^{*2} \, \mathrm{d}X \mathrm{d}Y \tag{2.37}$$

in time because the beta term is now orthogonal to Q^* (see Appendix B). A merit of considering (2.33) is that we can easily solve it by standard numerical methods (see Section 3). A disadvantage exists, however, in that it is, unlike (2.26), not derived in a systematic way from the original equations and needs some balancing condition. This is an ad hoc model, but it will be shown how it is capable of describing various physical phenomena.

2.3. *A comparison among various geostrophic models*

Table 1 compares the properties of various geostrophic equations recently derived mainly in the oceanographic context. All theories are distinguished from the view point of parameter constraints and global invariants. Charney-Flierl-Yamagata's equation governs a weakly nonlinear flow [$\varepsilon = O(s^2)$] in the intermediate scale between synoptic and planetary scale ($s \sim \beta \ll 1$) and conserves the total volume. The planetary geostrophic (PG_2) equation derived by Williams and Yamagata (1984) is of the same parameter constraint as here, but only conserves the total volume. Cushman-Roisin (1985) and Williams (1985) derive a general geostrophic equation which combines the quasi-geostrophic and intermediate scale dynamics. However, their equation is only valid for $s \sim O(1)$ because it merely conserves the total energy of the quasi-geostrophic form. The frontal geostrophic equation of Cushman-Roisin (1986) has a constraint such that it is restricted to the analyses of frontal motions. His equation also conserves the total volume and its higher order analogues. Salmon (1985) derives a new equation which is not restricted to a small deviation from a mean field and allows order one variations in Coriolis parameter and depth. As we have shown, Salmon's equation is equivalent to the energy-conserving potential vorticity equation for the intermediate scale motions. Furthermore (as shown in Appendix A), a special parameter constraint ($s \sim \beta \sim \varepsilon \ll 1$) allows us to study the dynamics in nearly physical space, not in the transformed coordinates. This has a practical advantage in numerical modelling. The numerical solutions of our new equation will be shown in Section 3.

3. Modelling of the cyclonic ring

3.1. *Observations*

Observations have shown that the Gulf Stream cyclonic rings are highly nonlinear mesoscale phenomena characterized by a large displacement of the isopycnals and the associated high Rossby number (typically characterized by the parameter range: $0.1 < \varepsilon \sim s < 1$). The rings have an interior core in near solid-body rotation

Table 1. *The properties of various geostrophic equations*

Ref.	Parameter constraint	Global invariants
Charney and Flierl (1981)		
Yamagata (1982)	$s \sim \beta \ll 1$; $\varepsilon = O(s^2)$	volume
Williams and Yamagata (1984)	$s \sim \beta \sim \varepsilon \ll 1$	volume
Cushman-Roisin (1985)		
Williams (1985)	$s = O(1)$, $\beta, \varepsilon \ll 1$	energy
Cushman-Roisin (1986)	$s = 0$, $\beta, \varepsilon \ll 1$	volume
Salmon (1985)		
eq. (2.26) here	$s \sim \beta \sim \varepsilon \ll 1$	energy
eq. (2.33) here	$s \sim \beta \sim \varepsilon \ll 1$	enstrophy

surrounded by a frontal jet exhibiting a maximum in the relative vorticity (Olson, 1980), and can take either circular or elliptic shape depending on their transit phase (Vestano et al., 1980). The beta number for the rings is so small ($\beta \sim 0.01$) that a short-time behavior is considered to be mainly controlled by the nonlinear advection process, although the β effect and diffusion process affect the propagation and decay of the rings during their long-time evolution (Cheney and Richardson, 1976; McWilliams and Flierl, 1979).

One of the intriguing motions the cyclonic rings show is the counter-clockwise rotation of its elliptical shape. Fig. 1 shows the shape evolution of cold core ring BOB during a period of 8 days. Spence and Legeckis (1981) estimated the period of rotation as about 18 days from a satellite-tracking data of BOB. Similar, but much slower, clockwise rotation is observed for the anticyclonic rings (e.g., see Cushman-Roisin et al., 1985). We are here concerned with a short-time evolution of the cyclonic ring shape. To see the degree to which we can accurately simulate the observational feature, we initialize with the ring shape which is considered to correspond to the satellite-observed one. We assume that the contour of maximum temperature gradient shown by the satellite data corresponds to that of maximum depth gradient in our model. For ring BOB, we choose the following parameter values:

$$f_0 = 9 \times 10^{-5}\,\mathrm{s}^{-1}, \quad \beta^* = 2 \times 10^{-11}\,\mathrm{m}^{-1}\,\mathrm{s}^{-1},$$

$$g^* = 0.02\ \mathrm{m/s}^2, \quad d_0 = 600\ \mathrm{m},$$

$$U = 1\,\mathrm{m/s}, \quad L = 60\,\mathrm{km} \tag{3.1}$$

The corresponding dimensionless numbers are given by

$$\beta = 0.01, \tag{3.2a}$$

$$\varepsilon = 0.2, \tag{3.2b}$$

$$s = 0.45. \tag{3.2c}$$

There are, of course, a number of assumptions and uncertainties which we cannot include in the simple parameter assumption (3.2). The first uncertainty arises from the value of s. The value $s = 0.45$ seems to be in the intermediate range between QG and IG regimes. For our theory to be a better model, it would be desirable that $s \sim 0.1$, at most. Therefore, the assumption (3.2c)

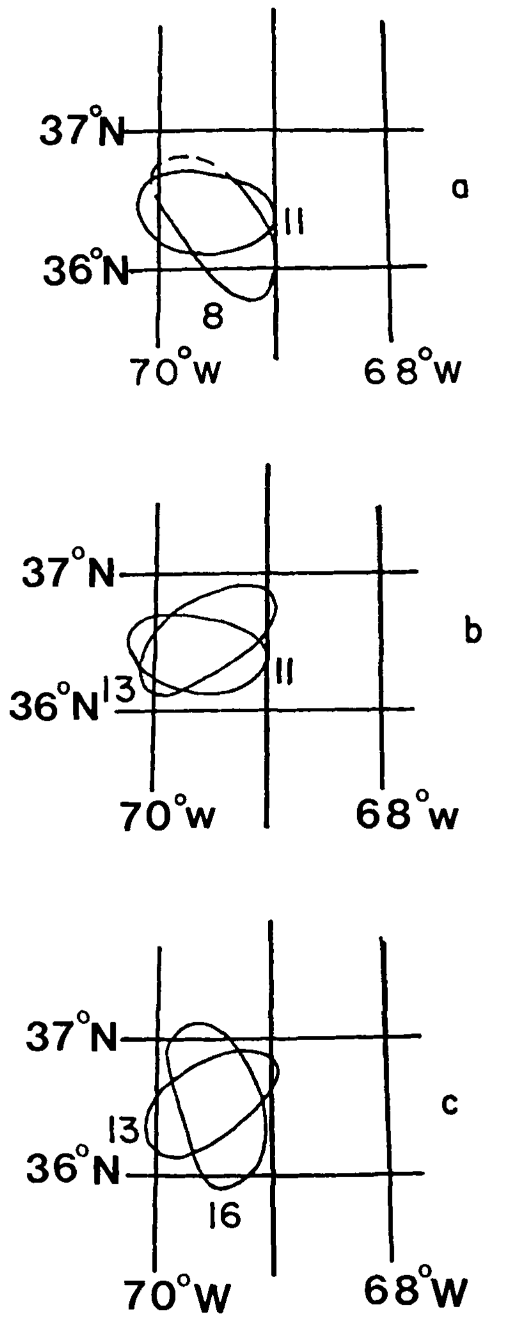

Fig. 1. A tracing of the BOB cyclonic ring for three intervals (days 8–11, 11–13, 13–16) during April 1977. The eddy outline corresponds to the position of the maximum surface temperature gradient as observed from satellite images. Adopted from Spence and Legeckis (1981).

could be the most severe error in modelling BOB. Another uncertainty occurs from the assumption on the vertical structure of BOB. The present model is built on highly simplified representation of baroclinicity. The Rossby number could also be a variable parameter. The value $\varepsilon = 0.2$ is chosen here because it best fits satellite observations [see Table 1 in Spence and Legeckis (1981)].

3.2. Numerical methods

We now consider the numerical solution of eq. (2.33) with (2.34) and (2.35). The remarkable feature of this system is that, although nonlinear, it can be reduced to the quasi-linear Helmholtz equation. To show this, we now let

$$w = \phi_t, \tag{3.3a}$$

$$d^* = s + \varepsilon\phi, \tag{3.3b}$$

$$G = d^* w. \tag{3.3c}$$

Rewriting (2.33) using (3.3) yields

$$\nabla^2 G - G/d^* = J(\phi, \pi^*). \tag{3.4}$$

Eq. (3.4) can be solved by using standard relaxation methods. The numerical procedure now looks easy. For the prescribed values of $\phi_{i,j,k}$, where the subscripts (i,j,k) denote the grid points of finite difference analogues of (x,y,t), one may solve (3.4) under the appropriate boundary conditions to find $G_{i,j,k}$. We then obtain $w_{i,j,k}$ from (3.3b, c). The leap-frog time difference formula for (3.3a) is next used to predict the values of $\phi_{i,j,k+1}$ at the next time step, provided $\phi_{i,j,k-1}$ is known. This procedure is repeated again and again. To avoid a numerical instability inherent to the leap-frog scheme, the ϕ-field is time-averaged between adjacent time steps at every n steps. The numerical integrations have shown that the solutions are rather insensitive to the value of n, while the potential enstrophy does not increase with time if we choose n sufficiently small (e.g., $n = 5$). Nonlinear aliasing is depressed by using Arakawa (1966)'s Jacobian form for the RHS in (3.4). The domain of integration is a 15×15 square with a fine mesh of 120×120 grid points and spacing $\Delta x = \Delta y = 0.125$, $\Delta t = 0.00625$. In all experiments, doubly periodic boundary conditions are used.

The initial condition is a somewhat troublesome problem. The radial structure of ring BOB does not seem to fit any simple profile of analytical functions (see Olson, 1980). Moreover, there is evidence that the ring was interacting with the Gulf Stream during this phase (Vastano et al., 1980). These observations make a hindcast using a simple ring model difficult. Nevertheless, it is still of considerable interest to examine a free evolution of the ring by using elementary functions for initial profiles. Thus, the ring profiles are modelled by the following:

$$\text{(I)}\ \phi(x,y,0) = -\exp[-\tfrac{1}{2}\rho^2], \tag{3.5a}$$

$$\text{(II)}\ \phi(x,y,0) = -\exp[-\tfrac{2}{3}\rho^3], \tag{3.5b}$$

Fig. 2 compares the two profiles, which are seemingly representative of the observed features as described by Olson (1980). The variable ρ is given through the relation:

$$\rho = r[p_0 - p_1 \cos 2(\theta - \theta_0)]^{1/2} \tag{3.5c}$$

where

$$r = (x^2 + y^2)^{1/2}, \qquad \theta = \tan^{-1}(y/x),$$

$$p_0 = (a^2 + b^2)/(2a^2 b^2), \qquad p_1 = (a^2 - b^2)/(2a^2 b^2).$$

We take $a = 1.5$, $b = 0.47$, $\theta_0 = 125°$ to fit the initial shape of BOB on day 8 in Fig. 1.

3.3. Results

We first examined a free evolution of profile (I). Fig. 3 shows the result. The degree of agreement between Fig. 1 and Fig. 3 is excellent. The more elongated shape of BOB on day 16 (Fig. 1c) may be attributable to the current-ring interaction (Vastano et al., 1980; Nof, 1985), which is absent in our model. A slight northward BOB movement during a period of 8 days may also be considered due to a similar mechanism. Apart from such slight differences between the data and model, a Gaussian profile gives a reasonably good result.

A question arises at this stage: what is the difference between the present and quasi-geostrophic models? We therefore looked at the evolution of BOB for exactly same conditions by solving the QG model (which is simply obtained by setting $\varepsilon = 0$ in the present model). Fig. 4 shows the result using the QG model. The initial BOB movement is not so different from Fig. 3. However, the difference is clearly visible at a later stage. The BOB asymmetric shape is gradually lost and becomes more circular. We thus conjecture that our equation is superior to the QG

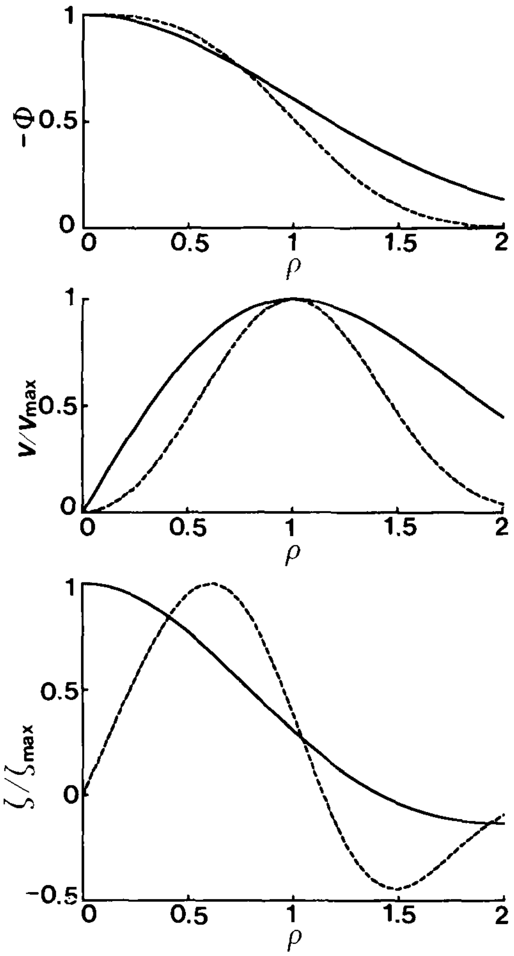

Fig. 2. A comparison of the radial structures of two profiles used for the model. The bold line represents the Gaussian profile (I) and the dotted line represents the cubic-Gaussian profile (II) in each figure. (a) Depth. (b) Velocity. (c) Relative velocity.

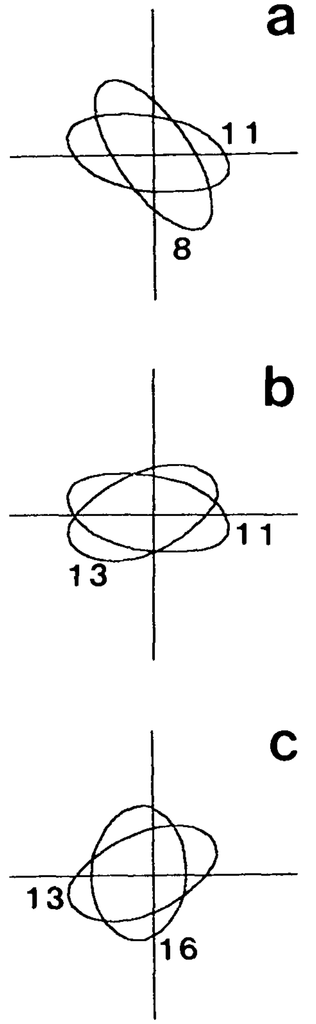

Fig. 3. A result solving eq. (2.33) for the Gaussian profile (I). The eddy outline corresponds to the position of the maximum depth gradient as calculated from the ϕ-field.

equation in the representation of the ring evolution characterized by high Rossby number.

We next examined the evolution of profile (II) for the same parameter values as in case (I). The result is shown in Fig. 5. The evolution in this case was quite different. The initial elliptical ring split into two cyclonic eddies, each inducing the anticyclonic ring on the northern and southern sides (day 3); then each began to separate (day 5), and the original cyclonic ring was transformed into two vortex pairs (day 8). The phenomenon is probably linked to barotropic instability, since the cubic-Gaussian eddy sharply changes sign with regard to the relative vorticity as shown in Fig. 2c. This result is consistent with the recent studies on frontal instability and formation of a dipole vortex (Griffiths and Linden, 1981; Flierl, 1985). The QG model for this case gives a qualitatively similar evolution.

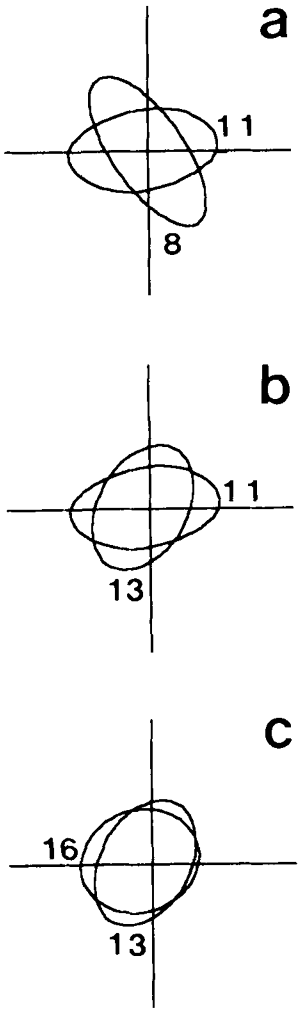

Fig. 4. Same as Fig. 3, but for the QG model.

4. Summary and discussion

We have derived a new geostrophic equation valid for the parameter range where Rossby, beta and stratification numbers are all small compared to unity. The derived equation conserves an analogue of either energy or enstrophy to higher orders of the Rossby number, and generalizes the previous studies on the IG dynamics. We have applied our equation to the cyclonic Gulf Stream ring BOB. The satellite data taken by Spence and Legeckis (1981) is compared with two initial profiles of BOB. The Gaussian profile gives a reasonably good agreement between the model and data: the initial elliptical ring rotates uniformly in a counterclockwise direction with a close similarity to the satellite image. The cubic Gaussian profile, however, reveals instability and splitting into two dipoles. This type of evolution is also probably observed for the oceanic eddies, where the relative vorticity sharply changes sign. We have looked at differences between the present and QG models. The QG model fails to predict the elliptical shape of BOB, while the present theory well describes the asymmetry during a period of 8 days.

The limitation of our model lies in the fact that it cannot describe baroclinic motions in a complete manner. Thus, it is of considerable interest to extend the theory to incorporate baroclinicity. In particular, a two-layer version of the present theory is worthy of further study. Furthermore, an interesting problem is to solve directly Salmon's equation and compare the solution with the present one. These problems are left to future work.

5. Acknowledgements

We are deeply grateful to an anonymous reviewer whose valuable comments significantly contributed to the improvement of our paper. The present study was supported by the Ministry of Education, Science and Culture of Japan through a Grant-in-Aid for General Scientific Research.

6. Appendix A

The forward and inverse transformations

The essence of the transformations used here is simply a strategy through which higher-order terms can be taken into considerations. The higher-order terms (often called errors) do not appear in a straightforward perturbation algorithm. One must therefore pay special attention to a problem which requires the exact conservation laws, the kind of problems which have been discussed by Salmon (1985), and studied here. The forward transformations are intended to find the missing terms and thus may be singular. There is no reason to look for higher-order terms

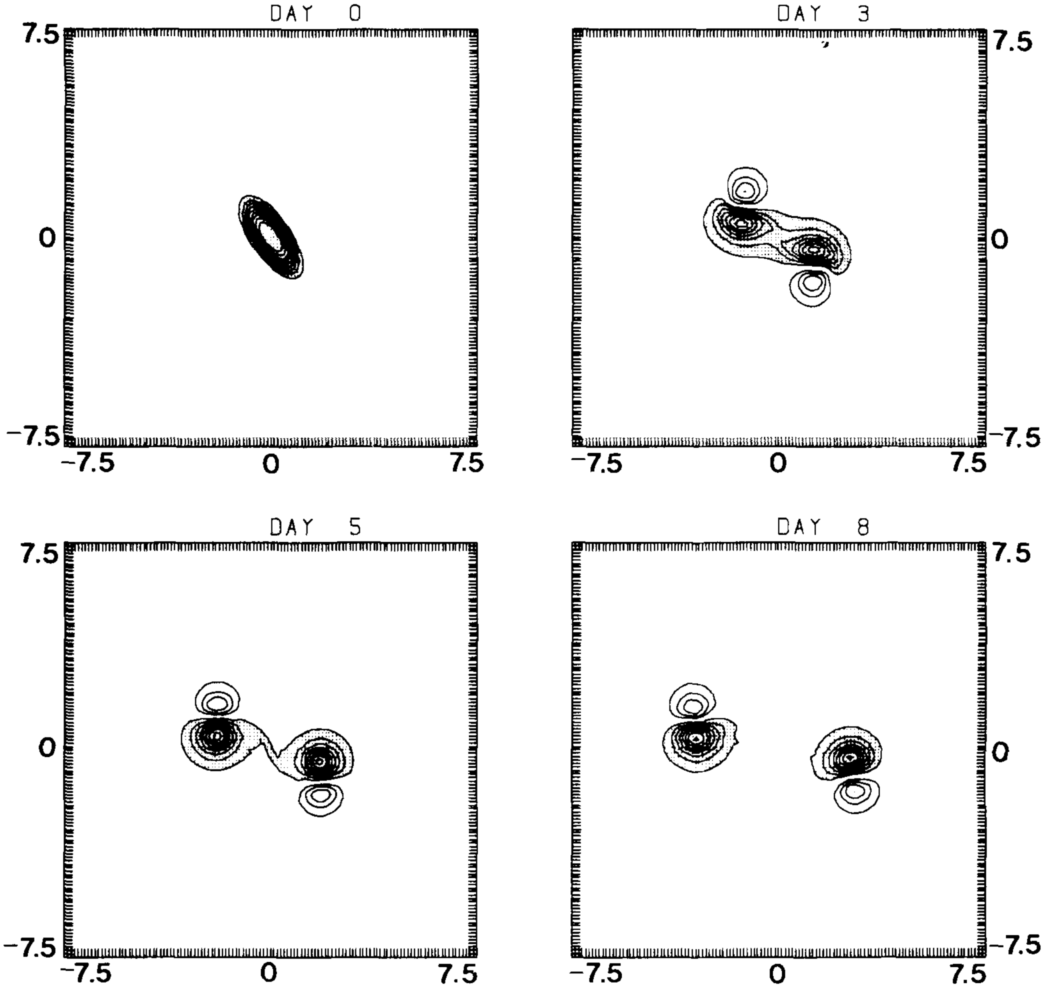

Fig. 5. The evolution of the cubic Gaussian profile (II). The contour interval between each streamline is 0.1. The shaded and non-shaded areas represent the cyclonic ($\phi < 0$) and anticyclonic ($\phi > 0$) regions, respectively.

once they have been recovered. Hence, the inverse transformation does not proceed in the same way as the forward transformation. Such definitions are obviously arbitrary, but a very useful conceptual means to analyze the present problem.

We now illustrate this by looking at the present situation. The approximate eq. (2.19) apparently lacks a term: $-\varepsilon\phi_t \nabla^2\phi$, which is a necessary part for time derivatives to be written as $\partial/\partial t$ of something. This term does not appear in (2.19) because of higher orders. The transformation (2.20) is now invoked to find the missing term. After using (2.21) and (2.22), it follows that we recover the missing term if the new equation is divided by $1 + \varepsilon\nabla^2\phi$, only leading terms in ε being kept in the equation. In this way we obtain eq. (2.23).

We next define the inverse transformation as

$$\left.\begin{aligned} \xi &= X - \varepsilon\phi_X, \\ \eta &= Y - \varepsilon\phi_Y, \\ \tau &= T, \end{aligned}\right\} \tag{A1}$$

and note that (ξ, η) differs from (x, y) by magnitudes of $O(\varepsilon^2)$. Thus the new coordinates are nearly identical to physical ones. Also note that

$$(\phi_X, \phi_Y, \phi_T) = (h_\xi, h_\eta, h_\tau). \tag{A2}$$

Thus, neglecting the errors of $O(\varepsilon^2)$, eq. (2.26) is back-transformed into

$$q_\tau + j(h, \pi) = 0, \tag{A3}$$

where

$$q = h - \frac{\varepsilon}{2}|\nabla h|^2 - (s + \varepsilon h)\nabla^2 h, \tag{A4}$$

$$\pi = q - (s + \varepsilon h)B\eta, \tag{A5}$$

with the definitions $\nabla = (\partial_\xi, \partial_\eta)$ and $j(a,b) = \partial(a,b)/\partial(\xi,\eta)$. Eq. (A3) is identical in form to eq. (2.26), but now expressed in a reference frame nearly identical to physical space. We can interpret (A3) as the potential vorticity equation which incorporates the ageostrophic effect in the advection term (see (2.18) in the text).

7. Appendix B

Proof of enstrophy conservation

Multiply (2.33) by Q^* and integrate over the entire region. Then, we have

$$F_t = 2B\langle Q^*(s + \varepsilon\phi)\phi_x\rangle, \tag{B1}$$

where $\langle\ \rangle$ means the surface integral over the entire domain. Using (2.34) for R.H.S. of (B1) and arranging it in powers of s and ε yields

$$F_t = -2B[s^2 C_1 + s\varepsilon(C_2 + C_3) + \varepsilon^2(C_4 + C_5)], \tag{B2}$$

where

$$\left.\begin{aligned} C_1 &= \langle \phi_x \nabla^2\phi\rangle \\ C_2 &= \langle 2\phi\phi_x \nabla^2\phi\rangle \\ C_3 &= \langle \phi_x |\nabla\phi|^2\rangle \\ C_4 &= \langle \phi^2\phi_x \nabla^2\phi\rangle \\ C_5 &= \langle \phi\phi_x |\nabla\phi|^2\rangle \end{aligned}\right\} \tag{B3}$$

After some simple algebra, it is shown that

$$\left.\begin{aligned} C_1 &= -\tfrac{1}{2}\langle |\nabla\phi|^2_x\rangle \\ C_2 &= -\langle \phi_x|\nabla\phi|^2\rangle = -C_3 \\ C_4 &= -\langle \phi\phi_x|\nabla\phi|^2\rangle = -C_5. \end{aligned}\right\} \tag{B4}$$

It follows that $C_1 = 0$, $C_2 + C_3 = 0$, $C_4 + C_5 = 0$, and thus, eq. (B2) proves the enstrophy conservation law $F_t = 0$.

REFERENCES

Arakawa, A. 1966. Computational design for long term numerical integration of the equation of fluid motion. Part 1. *J. Comput. Phys. 1*, 119–143.

Bolin, B. 1956. An improved barotropic model and some aspects of using the balance equation for three-dimensional flow. *Tellus 8*, 61–75.

Charney, J. G. 1948. On the scale of atmospheric motions. *Geophys. Pub. Norv. 17*, 1–17.

Charney, J. G. 1955. The use of the primitive equations of motion in numerical prediction. *Tellus 7*, 22–26.

Charney, J. G. and Flierl, G. R. 1981. Oceanic analogues of large-scale atmospheric motions. In *Evolution of physical oceanogrpahy* (eds. B. A. Warren and C. Wunsch). Massachusetts: MIT Press, 514–548.

Cheney, R. E. and Richardson, P. L. 1976. Observed decay of a cyclonic Gulf Stream ring. *Deep-Sea Res. 23*, 143–155.

Cushman-Roisin, B. 1985. *Towards a unified theory of geostrophic regimes*. A departmental report of the Geophysical Fluid Dynamics Institute at the Florida State University.

Cushman-Roisin, B., Heil, W. H. and Nof, D. 1985. Oscillations and rotations of elliptical warm-core rings. *J. Geophys. Res. 10*, 11756–11764.

Cushman-Roisin, B. 1986. Frontal geostrophic dynamics. *J. Phys. Oceanogr. 16*, 132–143.

Flierl, G. R. 1985. Instability of vortices. Woods Hole Oceanog. Inst. Tech. Rept. *WHOI-85-36*, 119 121.

Gent, P. R. and McWilliams, J. C. 1983a. Consistent balanced models in bounded and periodic domains. *Dyn. Atmos. Oceans 7*, 67–93.

Gent, P. R. and McWilliams, J. C. 1983b. Regimes of validity for balanced models. *Dyn. Atmos. Oceans 7*, 167–183.

Griffiths, R. W. and Linden, P. F. 1981. The instability of vortices in a rotating, stratified fluid. *J. Fluid Mech. 105*, 283–316.

Hoskins, B. J. 1975. The geostrophic momentum approximation and the semigeostrophic approximation. *J. Atmos. Sci. 32*, 233–242.

Leith, C. E. 1980. Nonlinear normal mode initialization and quasi-geostrophic theory. *J. Atmos. Sci. 37*, 958–968.

Lorenz, E. N. 1960. Energy and numerical weather prediction. *Tellus 12*, 364–373.

Lorenz, E. N. 1986. On the existence of a slow manifold. *J. Atmos. Sci. 43*, 1547–1557.

Matsuura, T. and Yamagata, T. 1982. On the evolution of nonlinear planetary eddies larger than the radius of deformation. *J. Phys. Oceanogr. 12*, 440–456.

McWilliams, J. C. and Flierl, G. R. 1979. On the evolution of isolated nonlinear vortices. *J. Phys. Oceanogr. 9*, 1155–1182.

Nof, D. 1985. On the ellipticity of isolated anticyclonic eddies. *Tellus 37A*, 77–86.

Olson, D. B. 1980. The physical oceanography of two rings observed by the Cyclonic Ring Experiments. Part II: Dynamics. *J. Phys. Oceanogr. 10*, 514–528.

Pedlosky, J. 1979. *Geophysical fluid dynamics*. New York: Springer-Verlag. 624 pp.

Salmon, R. 1985. New equations for nearly geostrophic flow. *J. Fluid Mech. 153*, 461–477.

Spence, T. W. and Legeckis, R. 1981. Satellite and hydrographic observations of low-frequency wave motions associated with a cold core Gulf Stream ring. *J. Geophys. Res. 86*, 1945–1953.

Vastano, A. C., Schmitz, J. E. and Hagan, D. E. 1980. The physical oceanography of two rings observed by the Cyclonic Ring Experiment. Part I: Physical structures. *J. Phys. Oceanogr. 10*, 493–513.

Williams, G. P. 1985. Geostrophic regimes on a sphere and a beta plane. *J. Atmos. Sci. 42*, 1237–1243.

Williams, G. P. and Yamagata, T. 1984. Geostrophic regimes, intermediate solitary vortices and Jovian eddies. *J. Atmos. Sci. 41*, 453–478.

Yamagata, T. 1982. On nonlinear planetary waves: a class of solutions missed by the quasi-geostrophic approximation. *J. Oceanogr. Soc. Japan 38*, 236–244.